© 2016. Published by The Company of Biologists Ltd | Journal of Experimental Biology (2016) 219, 2774 doi:10.1242/jeb.148197

CORRECTION

Correction: Separating underwater ambient noise from flow noise recorded on stereo acoustic tags attached to marine mammals

Alexander M. von Benda-Beckmann, Paul J. Wensveen, Filipa I. P. Samarra, S. Peter Beerens and Patrick J. O. Miller

There was an error published in *J. Exp. Biol.* **219**, pp. 2271-2275.

The units below Eqn 4 for p_{ref} are incorrect. The text should read: p_{ref}=1 µPa.

We apologise to the authors and readers for any inconvenience this may have caused.

Journal of Experimental Biology

© 2016. Published by The Company of Biologists Ltd | Journal of Experimental Biology (2016) 219, 2271-2275 doi:10.1242/jeb.133116

METHODS & TECHNIQUES

Separating underwater ambient noise from flow noise recorded on stereo acoustic tags attached to marine mammals

Alexander M. von Benda-Beckmann[1,*], Paul J. Wensveen[2], Filipa I. P. Samarra[2], S. Peter Beerens[1] and Patrick J. O. Miller[2]

ABSTRACT

Sound-recording acoustic tags attached to marine animals are commonly used in behavioural studies. Measuring ambient noise is of interest to efforts to understand responses of marine mammals to anthropogenic underwater sound, or to assess their communication space. Noise of water flowing around the tag reflects the speed of the animal, but hinders ambient noise measurement. Here, we describe a correlation-based method for stereo acoustic tags to separate the relative contributions of flow and ambient noise. The uncorrelated part of the noise measured in digital acoustic recording tag (DTAG) recordings related well to swim speed of a humpback whale (*Megaptera novaeangliae*), thus providing a robust measure of flow noise over a wide frequency bandwidth. By removing measurements affected by flow noise, consistent ambient noise estimates were made for two killer whales (*Orcinus orca*) with DTAGs attached simultaneously. The method is applicable to any multi-channel acoustic tag, enabling application to a wide range of marine species.

KEY WORDS: *Megaptera novaeangliae*, *Orcinus orca*, DTAG

INTRODUCTION

Sound-recording acoustic tags are commonly employed to study movement and acoustic behaviour of marine mammals (Marshall, 1998; Johnson and Tyack, 2003; Akamatsu et al., 2005; Goldbogen et al., 2006; Johnson et al., 2009), and are a key instrument in behavioural studies aimed at understanding the impact of anthropogenic sound (e.g. Tyack et al., 2011; Miller et al., 2012; Dunlop et al., 2013; Goldbogen et al., 2013). Acoustic tags are equipped with hydrophones to record vocalizations of the tagged and surrounding animals and other sound types such as exposure signals, e.g. sonar sounds or other control sounds (e.g. Tyack et al., 2011; Curé et al., 2012), or ambient noise. Ambient noise levels are of interest to efforts to understand the responsiveness of marine mammals to anthropogenic sound such as sonar signals or shipping noise (Ellison et al., 2012; Dunlop et al., 2013), or to estimate the communication space available to them (Miller, 2006; Clark et al., 2009). However, movement of the animal generates flow noise around the hydrophone (Haddle and Skudrzyk, 1969; Goldbogen et al., 2006), potentially masking other sounds at lower frequencies and limiting the capability to reliably measure ambient noise. Flow noise can also be exploited to estimate the animal's speed through the water (Goldbogen et al., 2006). Speed estimates can be used to obtain more accurate underwater movement paths via track-reconstruction methods (Wensveen et al., 2015), and are also used to indicate feeding attempts (lunges) of rorqual whales (Goldbogen et al., 2006; Doksæter Sivle et al., 2015).

Because of the turbulent nature of water flow around the receiving hydrophones, pressure fluctuations generated by the flow are uncorrelated between two hydrophones for frequencies higher than $f>(U/D)$, with D being the spacing of the two hydrophones and U the hydrophone speed through the water (Corcos, 1967). In contrast, ambient noise is correlated for $f\lesssim(1/10)c_s/D$, with c_s being sound speed in water (Cox, 1973). The relative contributions of flow and ambient noise can thus be estimated by calculating the coherence of the sound field measured on closely spaced hydrophones (e.g. Beerens et al., 1999; Barclay and Buckingham, 2013). This approach enables reliable measurements of ambient noise levels by removing data affected by flow noise, and provides a direct measurement of flow noise over a larger bandwidth than using a single hydrophone.

Here, we apply a correlation-based method to estimate the flow and ambient noise contributions in a recording made with acoustic version-2 digital sound recording tags (DTAGs) deployed on a humpback whale and two killer whales. DTAGs are commonly equipped with two hydrophones separated by 2.5 cm (Johnson et al., 2009), which theoretically can provide estimates of the contributions from flow and ambient noise for a frequency range between ∼0.1 and ∼6 kHz for an animal swim speed of 2.5 m s^{-1}.

MATERIALS AND METHODS

Acoustic tags

The acoustic tag used in this study was the version-2 DTAG; a suction-cup tag equipped with one or two hydrophones, depth and acceleration sensors (Johnson and Tyack, 2003; Johnson et al., 2009). The DTAGs sampled audio at 96 kHz (mn12_180a) or 192 kHz (oo09_144a/b) with 16-bit resolution, and had a flat frequency response with a 400 Hz one-pole high-pass filter. The acoustic sensitivity of the hydrophones, determined from calibration measurements, was −189±3 dB re. 1 μPa^{-1} (mean±s.d., N=3 tags) (P. J. Wensveen, Detecting, assessing, and mitigating the effects of naval sonar on cetaceans, Appendix III, PhD thesis, University of St Andrews, St Andrews, UK, 2016). These DTAGs were attached to a humpback whale and two killer whales during studies to investigate behavioural responses of marine mammals to sonar sounds (Miller et al., 2012; Doksæter Sivle et al., 2015) (Table S1). Animal experiments were carried out under permits issued by the Norwegian Animal Research Authority (permits S-2007/61201 and S-2011/38782), in compliance with ethical use of animals in experimentation. The research protocol was approved by the

[1]TNO Acoustics and Sonar, Oude Waalsdorperweg 63, The Hague 2597 AK, The Netherlands. [2]Sea Mammal Research Unit, Scottish Oceans Institute, University of St Andrews, Fife KY16 8LB, Scotland.

*Author for correspondence (sander.vonbenda@tno.nl)

A.M.v.B.-B, 0000-0002-4210-8058

Received 13 October 2015; Accepted 22 May 2016

Journal of Experimental Biology (2016) 219, 2271-2275 doi:10.1242/jeb.133116

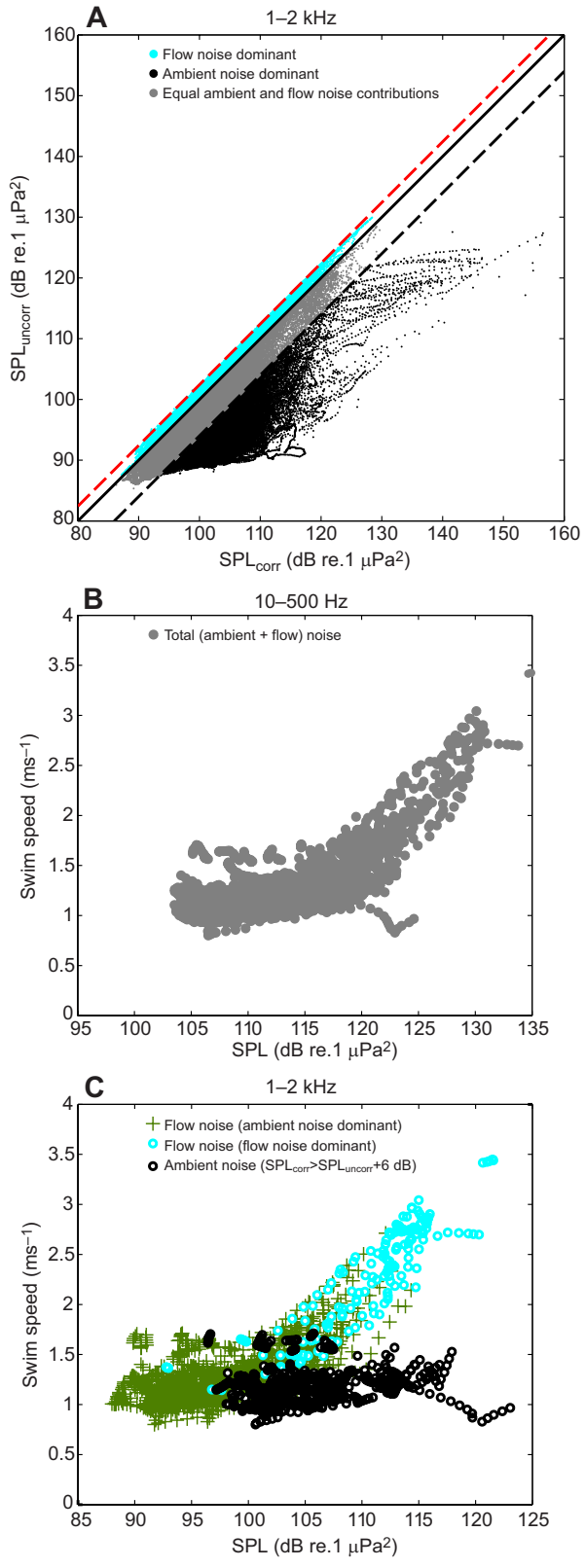

Fig. 1. Example of the relationship of sound pressure level (SPL) and animal swim speed. (A) SPLs measured in the frequency bands of 1–2 kHz for uncorrelated (SPL$_{uncorr}$) and correlated noise (SPL$_{corr}$). (B) Relationship between swim speed and total noise for the 10–500 Hz frequency band, commonly used to measure swim speed (Simon et al., 2012). (C) Relationship between swim speed and SPL$_{uncorr}$ and SPL$_{corr}$ in the 1–2 kHz frequency band. Cyan points in C were measured at times when SPL$_{uncorr}$>SPL$_{corr}$. Green crosses in C were measured at times when SPL$_{uncorr}$<SPL$_{corr}$. Data points (black circles in C and below black dashed line in A) for which SPL$_{corr}$>SPL$_{uncorr}$+6 dB were considered to be unaffected by flow noise, and a robust measure for ambient noise. The red dashed line in A indicates an empirically determined limit at which the coherence function could be measured when the uncorrelated flow noise levels exceeded the correlated noise levels, given by SPL$_{corr}$=SPL$_{uncorr}$+10 log$_{10}C_{lim}$dB. Here, the limit $C_{lim}=3/\sqrt{w\cdot T_{int}/2}$ was determined using the adopted bandwidth (w=200 Hz) and integration time (T_{int}=0.17 s) (see also Fig. S1). In C, measured SPL$_{uncorr}$ levels (green stars and cyan circles) on a tagged humpback whale, attributed to the flow noise, were strongly related (R^2=0.87) to forward swim speeds derived from the depth rate during high-pitch animal movements, even when the correlated part of the noise was greater than the uncorrelated part of the noise (green crosses). Noise segments where the correlated part of the noise was 6 dB or more greater than the uncorrelated part of the noise (black circles) had a low correlation with swim speed (R^2=0.17).

University of St Andrews Animal Welfare and Ethics Committee and the WHOI Institutional Animal Care and Use Committee.

Speed-through-water estimates of the humpback whale were derived from depth rate for periods when the animal was swimming at high absolute pitch (≥70 deg). Pitch angles were smoothed with a 5-s moving average filter to suppress effects of fluking motion.

Flow noise and ambient noise estimation

The contributions of the correlated and uncorrelated parts of the sound pressure on a pair of DTAG hydrophones (spaced 2.5 cm apart) were estimated. The spatial coherence function $C(f)$ was computed over small frequency bands:

$$C(f)=\frac{R_{12}}{\sqrt{R_{11}\cdot R_{22}}}, \quad (1)$$

with R_{lk} being the maximum amplitude of the band-pass filtered cross-spectral density:

$$R_{lk}=\max\left|\int_{f_c-w/2}^{f_c+w/2}(X_l(f)\cdot X_k^*(f))e^{-2\pi ift}\mathrm{d}f\right|, \quad (2)$$

with bandwidth w=200 Hz, l=1, 2 and k=1, 2 the hydrophone indices and f_c the center frequency. Here, $X(f)$ is proportional to the Fourier transform of the sound pressure, and $X^*(f)$ its complex conjugate, with $|X^2(f)|$ equal to the mean-square sound pressure spectral density (International Organization for Standardization, 2015), measured in a time window of 0.17 s.

The sound pressure level (SPL) of the correlated and uncorrelated parts of the signal was computed by integrating $X_1^2(f)$ over the frequency range $[f_{min}, f_{max}]$ of interest, and scaled by the correlated and uncorrelated contributions, respectively:

$$\mathrm{SPL}_{corr}=10\log_{10}\left(\frac{\int_{f_{min}}^{f_{max}}|X_1^2(f)|\cdot C(f)\mathrm{d}f}{p_{ref}^2}\right)\mathrm{dB}, \quad (3)$$

$$\mathrm{SPL}_{uncorr}=10\log_{10}\left(\frac{\int_{f_{min}}^{f_{max}}|X_1^2(f)|\cdot[1-C(f)]\mathrm{d}f}{p_{ref}^2}\right)\mathrm{dB}, \quad (4)$$

where p_{ref}=1 µm. The SPLs measured on a DTAG attached to a humpback whale were analyzed in the 1–2 kHz frequency band (the same band as the sonar transmissions in the controlled exposure experiments) for an 8 h period prior to the first sonar transmission. Subsets of noise measurements were created for

Journal of Experimental Biology (2016) 219, 2271-2275 doi:10.1242/jeb.133116

times during which: (1) $SPL_{uncorr}<SPL_{corr}$, and (2) $SPL_{corr}\geq SPL_{uncorr}+6$ dB (Fig. 1). The first subset was representative of flow noise even though correlated noise levels were higher, whereas the latter was unlikely to be affected by flow noise and was therefore representative of ambient noise. A 6 dB margin was adopted to account for uncertainties in the coherence measurement that are due to the short integration time [determined by measuring $C(f)$ for artificial time series consisting of coherent and incoherent Gaussian noise; Fig. S1]. The SPL measured from the humpback whale tag was filtered with a 5-s running average before comparing it with animal swim speed.

The two tagged killer whales were in close proximity of one another, allowing for cross-comparison of the estimated ambient noise. A 30-min period prior to the first sonar transmission was considered. Noise levels were expressed as SPLs, measured in 1/3-octave (decidecade; International Organization for Standardization, 2015) bands centred at 1 and 2 kHz. The ambient noise distribution for the killer whale tags was computed using data points at times where $SPL_{corr}\geq SPL_{uncorr}+6$ dB. We defined ambient noise as the contribution of all sound, except acoustic self-noise and transient sounds emitted by marine mammals and sonar. Thus, environmentally driven sound sources, such as breaking waves and rain, as well as continuous anthropogenic sound sources, such as shipping noise, were considered to contribute to the ambient noise. The correlated sound could contain contributions of transient sounds that were not considered as part of the ambient noise (Fig. 2). For instance, the 1–2 kHz band overlapped with the frequency range in which killer whales vocalize (Ford, 1989; Miller, 2006), and the sound of bubbles released during surfacing events. The start and end times for these sounds were manually selected for both tags. Noise segments that overlapped such transient signals were removed from the ambient noise analysis.

In all cases, data points for which the animal depth was less than 2 m were removed to avoid surface splashes affecting the measurements.

RESULTS AND DISCUSSION

Analysis of the humpback whale tag data showed that the uncorrelated part of the sound field, SPL_{uncorr}, at frequencies of 1–2 kHz was strongly related to swim speed (R^2=0.87; Fig. 1). This was similar to the correlation of the total SPL (R^2=0.86) in the 0.01–0.5 kHz band commonly used to derive swim speed from flow noise (e.g. Goldbogen et al., 2013) (Fig. 1). No clear relationship with swim speed (R^2=0.17) was found for data points where the correlated part of the sound field, SPL_{corr}, exceeded the uncorrelated part by more than 6 dB for the 1–2 kHz band. Those measurements were not affected by flow noise, and thus provided a measure of the ambient noise at the animal's location.

For the killer whale tags, high levels of flow noise were found to be more commonly present near 1 kHz than 2 kHz (Fig. 3, Table S2). A striking difference in flow noise levels was observed between the two tags. At 2 kHz, tag oo09_144b showed higher

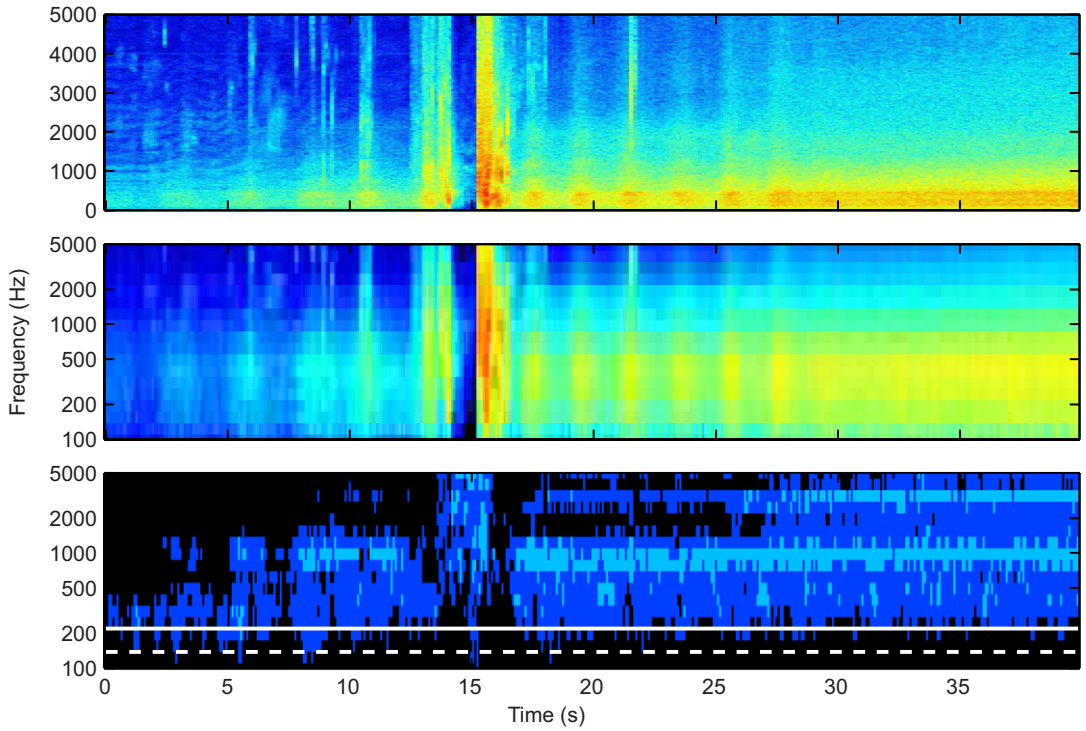

Fig. 2. Illustration of the flow noise rejection method. Top: An increase in flow noise can be seen in the DTAG audio recording as the killer whale (oo09_144a) broke the surface and actively stroked to increase speed while initiating a deep dive. The loud broadband sound around t=15 s were splashes that are due to the whale surfacing, which were rejected from the noise measurement by selecting times at which the animal was at depths greater than 2 m (the spectrogram was created by first downsampling the recorded signal by a factor of 10, and using an FFT window size of 1024 bins with a Hann window and 50% overlap). Middle: Same as top panel, but for 1/3-octave bands. Bottom: 1/3-octave band measurements for which the correlated noise, SPL_{corr}, exceeded the uncorrelated noise, SPL_{uncorr}, by more than 6 dB (black), and where $SPL_{uncorr}>SPL_{corr}$ (cyan). The cyan and blue areas therefore indicate measurements that were affected by flow noise, which clearly increased over a wider frequency range after the last surfacing when the animal sped up at the initiation of a deep dive. The white lines indicate the frequencies at which the theoretical coherence function of the flow noise has a value of $10\log_{10}C(f)=-6$ dB, assuming an animal swim speed of U=2.5 m s^{-1} (dashed line) and 4 m s^{-1} (solid line) (Corcos, 1967). Theory predicted that below these frequencies the signals generated by flow noise on the two hydrophone channels would be highly correlated, which was consistent with our observation of SPL_{corr} exceeding SPL_{uncorr} by 6 dB or more at low frequencies.

Journal of Experimental Biology (2016) 219, 2271-2275 doi:10.1242/jeb.133116

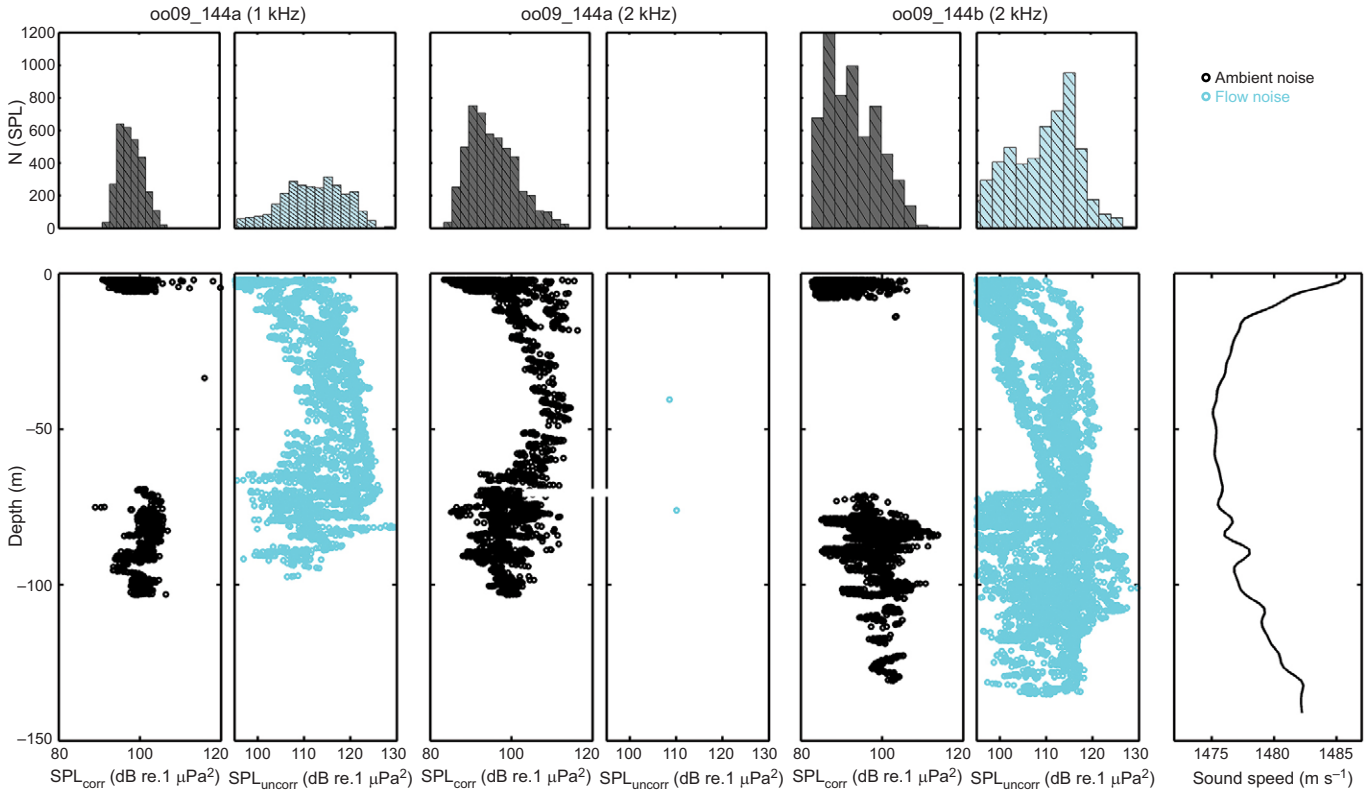

Fig. 3. Distributions and depth dependence of the ambient and flow noise. Shown are SPL in 1/3-octave bands centred at 1 kHz (left) and 2 kHz (middle) for ambient noise (black) and flow noise (cyan) contributions during a 30 min period for tag oo09_144a. The right panels show the 2 kHz levels for the other animal tag oo09_144b over the same time period. The rightmost bottom panel shows the sound speed profile that was obtained in the area on the same day. The upper panels show distributions of SPL during the 30 min period; below these panels are shown the depth dependence of the ambient noise levels. Only data points with depth >2 m were included, and where $SPL_{corr}>SPL_{uncorr}+6$ dB (black) and $SPL_{uncorr}>SPL_{corr}$ (cyan). Levels of flow noise in the 2 kHz band were high on tag oo09_144b, whereas flow noise levels rarely exceeded the ambient noise levels for tag oo09_144a. At depth, ambient noise levels on the two tags were within 2 dB (see Table S2), but at the surface levels for oo09_144b were roughly 4 dB lower than those for tag oo09_144a.

contributions of flow noise than tag oo09_144a, which was caused by a different location and orientation of the DTAG on the animal. Tag oo09_144a was positioned near the dorsal fin, but tag oo09_144b slid to the lower left side of the body soon after it was deployed (Fig. S2). The mean flow noise level was 10–19 dB higher than the mean ambient noise level (depending on the frequency and tag; Table S2). The total noise level measured on the DTAG therefore was not always a reliable measure of the ambient noise levels for these frequencies.

The ambient noise 1/3-octave band SPLs at 1 kHz ranged between 90 and 118 dB re. 1 µPa^2 (mean=96.3 dB re. 1 µPa^2, s.d.=3.4 dB), and at 2 kHz between 83 and 118 dB re. 1 µPa^2 (mean=96.7 dB re. 1 µPa^2, s.d.=5.7 dB). The ambient noise level was lower at the surface than at greater depths for both tagged animals. A clear increase in SPL_{corr} was observed as one animal (oo09_144a) dove between 20 and 60 m. Those maximum levels coincided with the depth at which the minimum sound speed was observed using CTD (SAIV SD200) measurements obtained in the same area (Fig. 3).

Wind-generated ambient noise is expected to be fairly constant with depth for these frequencies (Ainslie, 2010). The expected wind-generated 1/3-octave band SPLs at 1 and 2 kHz, for the conditions during the experiment (sea state 1; Miller et al., 2012), are 74 and 82 dB re. 1 µPa^2, respectively (Wenz, 1962). The mean ambient noise levels measured on the tags were approximately 15 to 22 dB above those predictions. Two vessels were known to be nearby during this period: MS Strønstad, at a distance between 40 and 300 m from the animals, and RV H. U. Sverdrup II, between 8 and 11 km distance. Locations of other vessels commonly present in the area were not measured. The lower levels near the surface and increase in noise as the animal passed through the acoustic channel indicated that ships were likely the dominant sound sources.

The ambient noise levels measured during deep dives (>20 m depth) were consistent between the two tagged killer whales, with mean values agreeing to within 2 dB. For shallow dives, the mean SPL_{corr} on tag oo09_144b was systematically lower by 3.8–7.1 dB than that on tag oo09_144a. Both animals showed little rolling behaviour during shallow dives. Because of the low placement of tag oo09_144b on the animal, body shielding of the ship noise could have led to consistently lower measured ambient noise levels (P. J. Wensveen, The effects of sound propagation and avoidance behaviour on naval sonar levels received by cetaceans, MPhil thesis, University of St Andrews, St Andrews, UK, 2012). Body shielding likely occurred occasionally for both animals during deeper dives where more rolling behaviour was observed, leading to more similar measured ambient noise levels during deep dives. These measured ambient noise levels are useful in the context of behavioural responses of killer whales to sonar, as they may be used to assess whether faint sonar signals were audible to the whales.

Our analysis demonstrated that estimated flow noise was strongly related to animal swimming speed even when the ambient noise levels exceeded the flow noise levels (Fig. 1). This confirmed that the uncorrelated part of the noise was caused by flow noise. By

removing time segments affected by flow noise, a realistic measure of ambient noise on DTAGs was obtained.

An important caveat is that this method worked in a limited frequency range. For low frequencies (roughly below 200 Hz), the sound pressure generated by flow noise on two DTAG hydrophones also became correlated (Fig. 2). The adopted integration time and bandwidth also limited the accuracy at which the coherence function could be measured. For the short time windows adopted here, the method required periods in the recordings during which the flow noise was substantially lower (≥6 dB) than the ambient noise, to estimate the ambient noise levels. This hindered measuring the contribution of ambient noise for low frequencies, which are of interest when investigating the effects of low frequency sound sources, such as shipping sound and airguns (e.g. Clark et al., 2009).

Ambient noise levels at even lower frequencies may be obtained by increasing the integration time, or placing two separate tags in close proximity on the same animal. An increase in integration time would allow for more reliable correlation measurements when flow noise dominates, at the expense of a decreased time resolution. A larger hydrophone separation would lower the frequencies at which flow noise becomes correlated (Corcos, 1967) and at which ambient noise becomes uncorrelated. Finally, future users should keep in mind that the dynamic range of recording systems can be limited by self-noise at the low end and that measuring very low ambient noise levels requires relatively sensitive hydrophones.

High flow noise levels, followed by a sudden strong decrease in flow noise levels, are used to acoustically detect lunge feeding attempts by baleen whales (Goldbogen et al., 2006, 2013; Simon et al., 2012; Doksæter Sivle et al., 2015). The low frequency band (typically <500 Hz) is used to detect lunges, as these provide a good proxy for flow noise (Simon et al., 2012) (Fig. 1). However, surfacing events as well as whale vocalizations also lead to strong peaks in low frequency noise. The flow noise separation method proposed in this study could improve the automatic detection of lunges, by providing a direct measure of the flow noise.

Acknowledgements
We gratefully acknowledge the 3S science team and the captains and crews of the MS Strønstad, and the RV H. U. Sverdrup II, for collecting data during the 3S studies. We thank Michael Ainslie for discussions and review of the manuscript, and the three anonymous reviewers, whose questions and comments significantly improved the manuscript. We further thank the sponsors, in particular René Dekeling (NL MoD) and Mike Weise (ONR), for supporting this work.

Competing interests
The authors declare no competing or financial interests.

Author contributions
A.M.v.B.-B. conceived the study, processed and analyzed DTAG data, and wrote the paper. P.J.O.M., P.J.W. and F.I.P.S. contributed to data collection and interpretation. S.P.B. provided the code for measuring the coherence function, and input on flow noise theory. P.J.W. analyzed animal swim speed, and carried out the DTAG calibration. F.I.P.S. and A.M.v.B.B. performed manual audits of the DTAGs for detecting transient sounds. All authors contributed to the manuscript editing.

Funding
A.M.v.B.B. and P.B. were funded by The Netherlands Ministry of Defence. Fieldwork efforts and support for P.M. and F.S. was provided by the US Office of Naval Research [award numbers N00014-08-1-0984 and N00014-10-1-0355]. P.W. received a PhD studentship with matched funding from The Netherlands Ministry of Defence (administered by The Netherlands Organisation for Applied Scientific Research, TNO) and UK Natural Environment Research Council [NE/J500276/1].

Supplementary information
Supplementary information available online at
http://jeb.biologists.org/lookup/doi/10.1242/jeb.133116.supplemental

References
Ainslie, M. A. (2010). *Principles of Sonar Performance Modeling*, 707 pp. Berlin: Springer Verlag.
Akamatsu, T., Matsuda, A., Suzuki, S., Wang, D., Wang, K., Suzuki, M., Muramoto, H., Sugiyama, N., Oota, K. (2005). New stereo acoustic data logger for free-ranging dolphins and porpoises. *J. Mar. Tech. Soc.* **39**, 3-9.
Barclay, D. R. and Buckingham, M. J. (2013). The depth-dependence of rain noise in the Philippine Sea. *J. Acoust. Soc. Am.* **133**, 2576-2585.
Beerens, S. P., van IJssemuide, S. P., Volwerk, C., Doisy, Y., and Trouve, E. (1999). Flow noise analysis of towed sonar arrays. UDT 99-Conference Proceedings Undersea Defense Technology, June 29-July 1, 1999, Nice, France, Nexus Media Limited, Swanley, Kent.
Clark, C. W., Ellison, W. T., Southall, B. L., Hatch, L., Van Parijs, S. M., Frankel, A. and Ponirakis, D. (2009). Acoustic masking in marine ecosystems: intuitions, analysis, and implication. *Mar. Ecol. Prog. Ser.* **395**, 201-222.
Corcos, G. M. (1967). The resolution of turbulent pressures at the wall of a boundary layer. *J. Sound Vib.* **6**, 59-70.
Cox, H. (1973). Spatial correlation in arbitrary noise fields with application to ambient sea noise. *J. Acoust. Soc. Am.* **54**, 1289-1301.
Curé, C., Antunes, R., Samarra, F., Alves, A. C., Visser, F., Kvadsheim, P. H. and Miller, P. J. O. (2012). Pilot whales attracted to killer whale sounds: acoustically-mediated interspecific interactions in cetaceans. *PLoS ONE* **7**, e52201.
Doksæter Sivle, L., Kvadsheim, P. H., Curé, C. Isojunno, S., Wensveen, P. J., Lam, F.-P. A., Visser, F., Kleivane, L., Tyack, P. L., Harris, C. M. et al. (2015). Severity of expert-identified behavioural responses of humpback whale, mike whale, and northern bottlenose whale to naval sonar. *Aquat. Mamm.* **41**, 469-502.
Dunlop, R. A., Noad, M. J., Cato, D. H., Kniest, E., Miller, P. J. O., Smith, J. N. and Stokes, M. D. (2013). Multivariate analysis of behavioural response experiments in humpback whales (*Megaptera novaeangliae*). *J. Exp. Biol.* **216**, 759-770.
Ellison, W. T., Southall, B. L., Clark, C. W. and Frankel, A. S. (2012). A new context-based approach to assess marine mammal behavioral responses to anthropogenic sounds. *Conserv. Biol.* **26**, 21-28.
Ford, J. K. B. (1989). Acoustic behaviour of resident killer whales (*Orcinus orca*) off Vancouver Island, British Columbia. *Can. J. Zool.* **67**, 727-745.
Goldbogen, J. A., Calambokidis, J., Shadwick, R. E., Oleson, E. M., McDonald, M. A. and Hildebrand, J. A. (2006). Kinematics of foraging dives and lunge-feeding in fin whales. *J. Exp. Biol.* **209**, 1231-1244.
Goldbogen, J. A., Southall, B. L., DeRuiter, S. L., Calambokidis, J., Friedlaender, A. S., Hazen, E. L., Falcone, E. A., Schorr, G. S., Douglas, A., Moretti, D. J. et al. (2013). Blue whales respond to simulated mid-frequency military sonar. *Proc. R. Soc. B* **280**, 20130657.
Haddle, G. P. and Skudrzyk, E. J. (1969). The physics of flow noise. *J. Acoust. Soc. Am.* **46**, 130-157.
International Organization for Standardization (2015). ISO/DIS 18405 Underwater Acoustics – Terminology. Geneva: International Organization for Standardization.
Johnson, M. P. and Tyack, P. L. (2003). A digital acoustic recording tag for measuring the response of wild marine mammals to sound. *IEEE J. Oceanic Eng.* **28**, 3-12.
Johnson, M., Aguilar de Soto, N. and Madsen, P. T. (2009). Studying the behaviour and sensory ecology of marine mammals using acoustic recording tags: a review. *MEPS* **395**, 55-73.
Marshall, G. J. (1998). CRITTERCAM: an animal borne imaging and data logging system. *Mar. Technol. Soc. J.* **32**, 11-17.
Miller, P. J. O. (2006). Diversity in sound pressure levels and estimated active space of resident killer whale vocalizations. *J. Comp. Physiol. A* **192**, 449-459.
Miller, P. J. O., Kvadsheim, P. Lam, F. P. A. Wensveen, P. J. Antunes, R. Alves, A. C. Visser, F., Kleivane, L. Tyack, P. L. and Doksæter Sivle, L. (2012). The severity of behavioral changes observed during experimental exposures of killer (*Orcinus orca*), long-finned pilot (*Globicephala melas*), and sperm whales (*Physeter macrocephalus*) to naval sonar. *Aquat. Mamm.* **38**, 362-401.
Simon, M., Johnson, M. and Madsen, P. T. (2012). Keeping momentum with a mouthful of water: behavior and kinematics of humpback whale lunge feeding. *J. Exp. Biol.* **215**, 3786-3798.
Tyack, P. L., Zimmer, W. M. X., Moretti, D., Southall, B. L., Claridge, D. E., Durban, J. W., Clark, C. W., D'Amico, A., DiMarzio, N., Jarviset, S. (2011). Beaked whales respond to simulated and actual navy sonar. *PLoS ONE* **6**, e17009.
Wensveen, P. J., Thomas, L. and Miller, P. J. O. (2015). A path reconstruction method integrating dead-reckoning and position fixes applied to humpback whales. *Mov. Ecol.* **3**, 31.
Wenz, G. M. (1962). Acoustic ambient noise in the ocean: spectra and sources. *J. Acoust. Soc. Am.* **34**, 1936-1956.

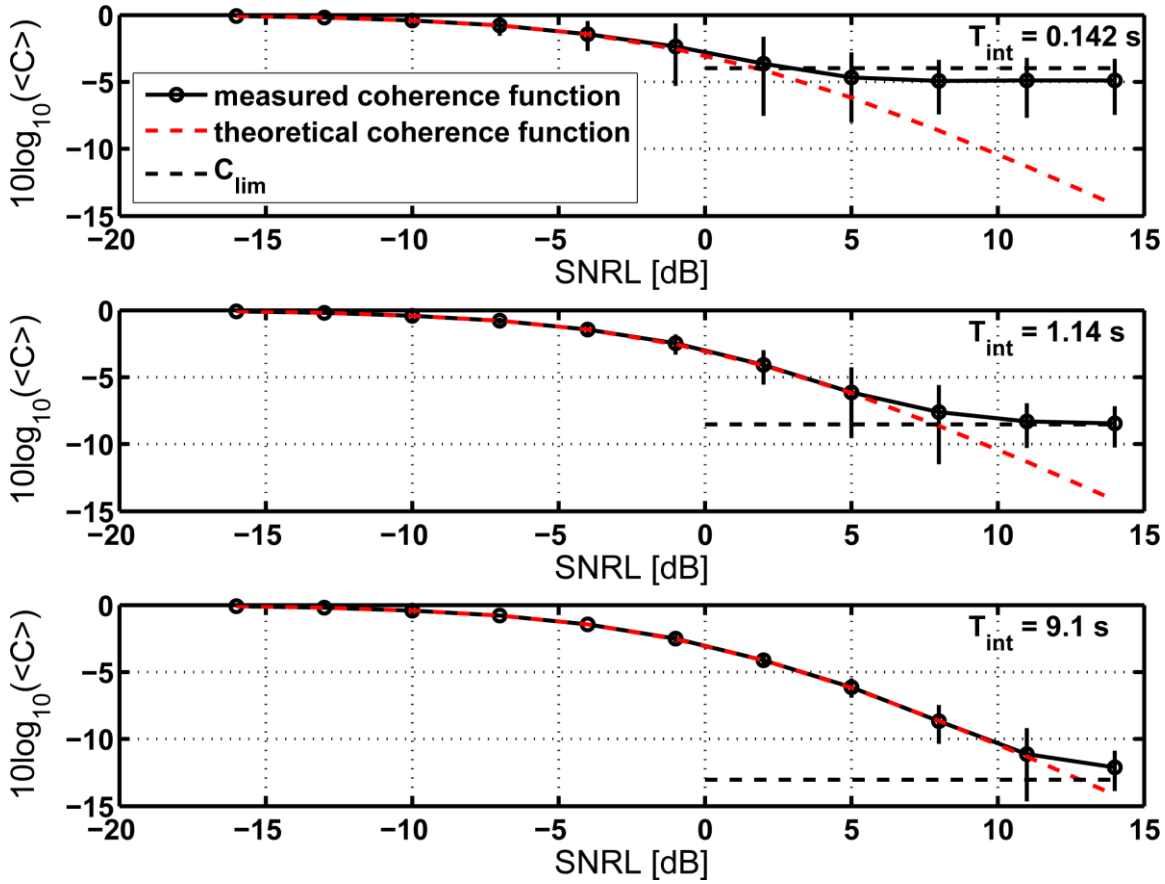

Fig. S1. Accuracy of the measured mean coherence function for an integration time of 0.14 s (top), 1.14 s (middle), and 9.1 s (bottom) for random Gaussian noise. The accuracy of the measured mean coherence function <C>, averaged over all frequencies, as a function of SNRL = $SPL_{ncorr} - SPL_{corr}$, with the correct coherence coefficient superimposed in red. Artificial time series were generated by mixing a coherent and incoherent time series. Error-bars indicate the 3-sigma uncertainties on the measured mean coherence function. The black dashed line shows the empirically determined limit $C_{\mathrm{lim}} = \frac{3}{\sqrt{N_{\mathrm{samp}}/2}}$ for measuring the coherence function when the flow noise dominates, with $N_{\mathrm{samp}} = \frac{w}{df} = w \cdot T_{\mathrm{int}}$ and df the frequency resolution. The shortest integration time (0.14 s, top panel) indicated that in order

to ensure that the measurement was dominated by the correlated noise (SNRL ≤ -3 dB), the measured level of the correlation coefficient $10 \log_{10} \langle C \rangle$ needed to be at least -6 dB or higher. This criterion was adopted to obtain reliable measurements of the ambient noise. For the longest integration time (9.1 s, bottom panel), the correlation coefficient could be measured reliably even when the uncorrelated noise exceeded the correlated noise by 10 dB.

Fig. S2. Tag placement location on two killer whales. The top picture shows the tag placement of oo09_144a, and the bottom picture that of oo09_144b. Tag oo09_144b was situated on the left flank of the killer whale, whereas tag oo09_144a was placed just posterior

of the dorsal fin of the animal. Tag oo09_144a was positioned on the right side of the body near the dorsal fin and slid backwards slightly during the deployment. The tag on the other animal slid much further down, to the lower left side of the body, soon after it was deployed. Before the start of the first sonar exposure, the tagged animals were making deep dives, with underwater tail slap sounds indicative of feeding recorded on the tags.

Table S1. Stereo acoustic version-2 DTAG deployments on two whale species. The table lists the tags used in the flow and ambient noise analysis, with Tag ID, species, estimated age/sex of the animals, dates, duration and general area of the tag deployments.

Tag ID	**Species**	**Age/Sex**	**Date**	**Deployment duration**	**Location**
mn12_180a	Humpback whale (*Megaptera novaeangliae*)	adult female	June 2012, at 18:03 UTC	15 hours	Near Bear Island
oo09_144a	Killer whale (*Orcinus orca*)	adult male	May 2009 at 09:58 UTC	12 hours	Norwegian continental shelf (Vesteralen area)
oo09_144b	Killer whale (*Orcinus orca*)	adult male	May 2009 at 10:52 UTC	12 hours	Norwegian continental shelf (Vesteralen area)

Table S2. Measured contribution of correlated and uncorrelated noise on total noise budget. Listed are the total sound pressure levels (SPL) measured in different depth ranges for different frequencies measured on two tagged killer whales (oo99_144a, oo09_144b) during a 30 min period. The table shows the mean (+/-1 SD) of the SPL_{tot} for all data points, and mean (+/- 1 SD) for times when the correlated part dominated the sound field (SPL_{corr}) and for when the uncorrelated dominated the correlated contribution (SPL_{uncorr}). The fractions of time of which the correlated or uncorrelated noise dominated the noise level are indicated in separate columns. The SPL_{corr} (indicated in bold) was considered to provide a reliable estimate of the ambient noise during the 30 min period.

Frequency	**Depth range [m]**	**total <SPL$_{tot}$> dB re 1 µPa^2 (+/- 1 SD)**	**correlated <SPL$_{corr}$> dB re 1 µPa^2 (+/- 1 SD)**	**Fraction of time correlated noise dominant**	**uncorrelated <SPL$_{uncorr}$> dB re 1 µPa^2**	**Fraction of time uncorrelated noise dominant**
Oo09_144a						
1 kHz (1/3 Oct)	2 – 20	100.2 (± 6.4)	**96.8 (± 2.5)**	0.31	106.8 (±6.9)	0.07
	20 – 400	110.6 (± 8.1)	**100.8 (±2.6)**	0.24	113.7 (±6.0)	0.63
2 kHz (1/3 Oct)	2 – 20	94.1 (±6.2)	**92.8 (±5.1)**	0.44	n/a	0
	20 – 400	104.0 (±7.0)	**99.7 (±4.9)**	0.61	109.3 (±1.1)	0.0005

Oo09_144b						
1 kHz (1/3 Oct)	2 – 20	97.5 (±10.9)	**88.7 (±3.5)**	0.13	105.2 (±8.9)	0.17
	20 – 400	116.8 (±10.3)	**100.4 (±3.2)**	0.14	119 (±7.6)	0.79
2 kHz (1/3 Oct)	2 – 20	92.0 (± 6.7)	**89.0 (± 3.7)**	0.20	98.0 (±7.2)	0.06
	20 – 400	107.8 (±9.2)	**98.0 (±5.2)**	0.25	110.6 (±7.1)	0.45